International Journal of Engineering

Journal Homepage: www.ije.ir

Prediction of Hardness of Copper-based Nanocomposites Fabricated by Ball-milling using Artificial Neural Network

R. M. Babaheydari[a], S. O. Mirabootalebi*[a,b], G. H. Akbari[a], H. Salehifar[c]

[a] *Department of Materials & Metallurgy, Faculty of Engineering, Shahid Bahonar University of Kerman, Kerman, Iran*
[b] *College of Science and Engineering, James Cook University, Townsville, Queensland, Australia*
[c] *Department of Computer Science and Automation, Technical University of Ilmenau, Germany*

PAPER INFO

Paper history:
Received 16 June 2023
Received in revised form 21 July 2023
Accepted 23 July 2023

Keywords:
Copper Nanocomposites
Copper Alloys
Mechanical Alloying
Artificial Neural Network
Prediction Micro-hardness
Mechanical Properties

ABSTRACT

Copper-based alloys are one of the most popular materials in the power distribution, welding industry, hydraulic equipment, industrial machinery, etc. Among different methods for the fabrication of Cu alloys, mechanical alloying (MA) is the major approach due to the fact that this approach is simple, inexpensive, suitable for mass production, and has a high capacity for homogeneous distribution of the second phase. However, the prediction of the hardness of products is very difficult in MA because of a lot of effective parameters. In this work, we designed a feed-forward back propagation neural network (FFBPNN) to predict the hardness of copper-based nanocomposites. First, some of the most common nanocomposites of copper including Cu-Al, Cu-Al_2O_3, Cu-Cr, and Cu-Ti were synthesized by mechanical alloying of copper at varying weight percentages (1, 3, and 6). Next, the alloyed powders were compacted by a cold press (12 tons) and subjected to heat treatment at 650˚C. Then, the strength of the alloys was measured by the Vickers microscopy test. Finally, to anticipate the micro-hardness of Cu nanocomposites, the significant variables in the ball milling process including hardness, size, and volume of the reinforcement material, vial speed, the ball-to-powder-weight-ratio (BPR), and milling time; were determined as the inputs, and hardness of nanocomposite was assumed as an output of the artificial neural network (ANN). For training the ANN, many different ANN architectures have been employed and the optimal structure of the model was obtained by regression of 0.9914. The network was designed with two hidden layers. The first and second hidden layer includes 12 and 8 neurons, respectively. The comparison between the predicted results of the network and the experimental values showed that the proposed model with a root mean square error (RMSE) of 3.7 % can predict the micro-hardness of the nanocomposites.

***doi**: 10.5829/ije.2023.36.10a.17*

1. INTRODUCTION

Nanocomposites and advanced materials have a widespread application in various fields, and based on the production methods, there are different generation strategies [1-3]. Adding alloying elements to the copper lattice is a common way to increase the mechanical properties alongside the electrical properties of copper-based composites. In other words, copper alloys are able to strengthen without a major decrease in their electrical properties [4, 5]. The creation of a saturated solid solution and the nano-sized precipitations in the copper lattice is a desirable method to increase the toughness, tensile strength, creep resistance, and thermal stability of Cu with negligible reduction in the electrical conductivity [6, 7]. Except for Cu-Be, different copper-based alloys are being developed. Cu-Ti alloy is a striking example, which is a favorable alternative for Cu-Be. In general, Cu composites have proper strength, excellent electrical conductivity, high corrosion resistance, and suitable thermal stability [8, 9]. Likewise, each of the Cu-based composites has various applications. For instance, Cu–Al in solar powers and memory alloys [10], Cu-Al_2O_3 in

*Corresponding Author Email: oveis@eng.uk.ac.ir
(S. O. Mirabootalebi)

Please cite this article as: R. M. Babaheydari, S. O. Mirabootalebi, G. H. Akbari, H. Salehifar, Prediction of Hardness of Copper-based Nanocomposites Fabricated by Ball-milling using Artificial Neural Network, ***International Journal of Engineering, Transactions A: Basics***, Vol. 36, No. 10, (2023), 1932-1941

electrodes [11], Cu-Cr in fuel cells [12], and Cu-Ti in solar cells [13]; are being used.

The common methods for fabrication copper composites including in-situ reduction [14], melting and casting [15, 16], electrolysis [17], hydrothermal [18], severe plastic deformation (SPD) [19], sol-gel [20, 21], accumulative roll-bonding (ARB) [22], and high-energy ball milling [5, 23]. Among these approaches, mechanical alloying is a simple, inexpensive, and environmental-friendly process with the uniform dispersion of the alloying elements and has been widely used for the fabrication of advanced materials and nanocomposites [24, 25].

The effective parameters during the milling process influence various properties of Cu nanocomposites, especially the micro-hardness. The wrong combination of the MA parameters leads to an undesirable product and disrupts the balance between the electrical and mechanical properties of Cu-based nanocomposites. The exact determination of the micro-hardness of Cu-based composites results in the optimal usage of the process for the widespread synthesizing of copper nanocomposites.

There are several numerical analyses for the prediction of desirable output and optimization of the process, such as ANN [26], Genetic Algorithm [5], and Taguchi [27, 28]. ANN owing to its high capacity for the classification of big data, reaching a trusted solution, and approaching various variables, is a powerful machine learning approach for the prediction of outputs [29-31]. This method could be used as a parallel process with non-linear handling and adaptability which has a high capability to analyze various factors (noisy data) to predict the outputs. As a result, the artificial neural network is widely used in mechanical alloying owing to various major factors and the stochastic nature of the MA. The mechanism of ANN is also relatively simple and is based on training and then the anticipation of output. Nevertheless, no previous study has investigated a comprehensive model for the anticipation of the hardness of the main copper composites.

In this study, Cu-Al, Cu-Al_2O_3, Cu-Cr, and Cu-Ti with different percentages of the reinforcement elements were produced by MA. Then, the generated Cu composites were analyzed by X-ray powder diffraction (XRD) and scanning electron microscopy (SEM). Afterward, the sintering process was carried out and the micro-hardness of the Cu solid solutions was investigated via a Vickers hardness tester. Lastly, the obtained hardness data were used to design an ANN for predicting the micro-hardness of Cu-nanocomposites.

2. ANN MODELING

ANN is based on the intelligent creatures learning procedure containing interrelated cells called nodes or neurons. They are the basic computational units that are linked together through the signals. The signals aggregate into layers and signal transmission between input and output is performed several times [32]. ANN is constructed of the input, hidden, and output layers. The learning process of a neural network includes regulating the neuron's bias, altering the weights, and output normalization via the transfer functions. The process of the training process will be extended till the ANN network reach near the favorable output and attain a reasonable percentage error.

The mathematical equation of an artificial neural network is able to be extracted from the mentioned component including biases, weights, transfer functions, and neurons. The connection between neurons is defined by Equation (1):

$$x = \sum_{i=1}^{p} w_i x + b \quad (1)$$

where x is the output and p is the number of components in the layer. $w_i x$ and b are the weight and bias, respectively.

3. EXPERIMENTAL

High-purity flakes of copper, chromium, aluminum, alumina, and titanium were chosen as the precursors. Specimens with different weight percentages of the second phase (1, 3, and 6) were mechanically alloyed in a planetary ball mill under the Argon. Two sizes of balls (15 and 10 mm in diameter) were used and BPR was kept at 15:1. The primary raw material was copper powders (15 g). Cu-Al and Cu-Al_2O_3 were milled for 40 h and the activation time for Cu-Ti and Cu-Cr was 90 h at a vial speed of 350 rpm. The selection of milling times was based on the experience of similar studies for the creation of the solid solution of Cu alloys.

A Philips X'PERT MPD (Cu-Kα) was used to analyze the crystallographic structures of samples. Morphology and size of Cu particles were studied by SEM (Cam Scan mv2300). For the annealing of the specimens, the alloying powders were molded to a thickness of 1 mm and a diameter of 1 cm. 1.4 g of samples were have been pressed by an automatic powder cold press machine (12 tons). The annealing process was applied in a simple heat treatment oven for 30 minutes at 650˚C under Argon atmosphere. The Vickers hardness testing was carried out as stated in the ASTM International Standards (E-348-89) and hardness was monitored by an impression of a load (98.7 mN) which is applied smoothly for 5 s at high magnification.

4. RESULTS AND DISCUSSION

The XRD patterns of Cu-based solid solutions after the mechanical alloying are shown in Figure 1. It is very

significant to confirm the creation of XRD patterns of Cu-based solid solutions. In the MA process, all of the particles are rigorously distorted through the collision of the balls which causes a rise in the atomic diffusion and regional temperature [33]. The solubility of alloying elements in Cu is increased by raising the temperature. Simultaneously, the concentration of crystallographic defects (dislocations, stacking faults, and vacancies) was significantly developed throughout the MA. Consequently, the flakes become work-hardened after a while, and the width of peaks was also enhanced by the rise in the work-hardening of the micro-strain [9]. Growth in weight percentage of the second phase brings on the height reduction and width broadening of the XRD profiles, as well as, peaks shifting to lower angles (except Cu-Al_2O_3). Chromium, titanium, and aluminum have a larger atomic size than Cu. Thus, the disintegration of the reinforced materials and increasing concentration in the copper lattice rise the lattice constant of copper and move the X-ray diffraction patterns to the left. The non-movement of the major peaks of Cu in the XRD patterns of Al_2O_3 illustrates that the particles of alumina were not dissolved within the copper lattice.

The morphology of the samples is depicted in Figures 2-5. The particle size of Cu-Al alloys is declined by proportion enhancement in Al_2O_3. Generally, particles are soft at the start of the MA, although, they were welded together and tend to agglomeration during the mechanical alloying [34]. The reduction of powder particle size of Al_2O_3 follows two distinct mechanisms.

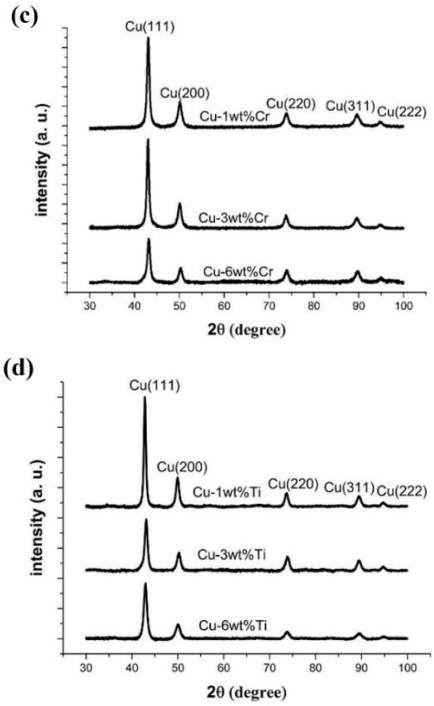

Figure 1. XRD of Cu-Al (a), Cu- Al_2O_3, Cu-Cr, and Cu-Ti nanocomposites prepared by MA

First, through incorporating the Cu particles. Second, by increasing the strain of the lattice via fracturing the

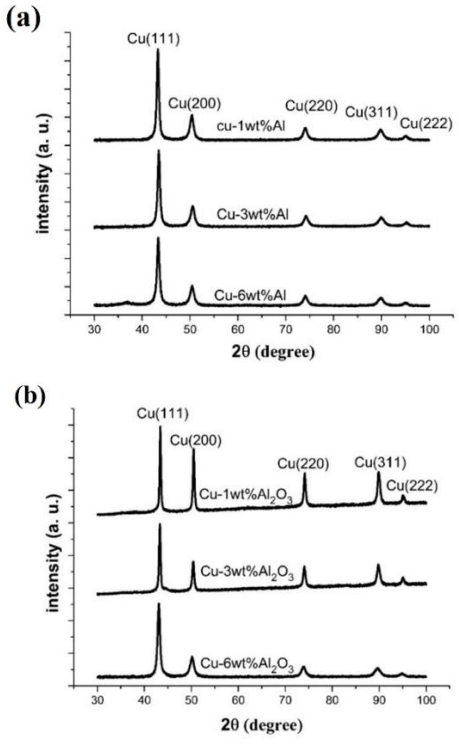

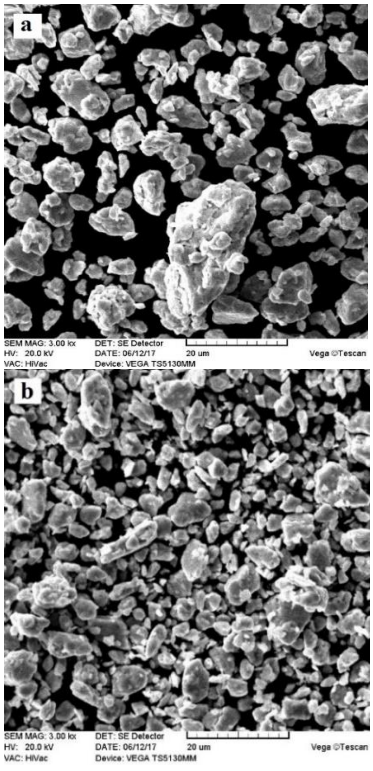

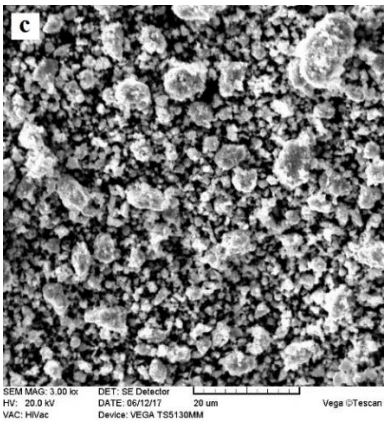

Figure 2. SEM images of Cu-Al alloys with 1, 3, and 6 weight percentages

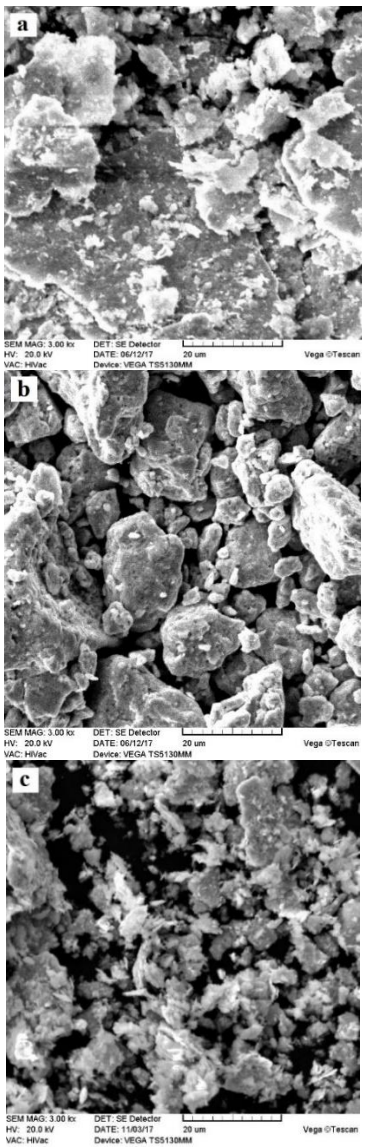

Figure 3. SEM images of Cu-Al_2O_3 samples with 1, 3, and 6 weight percentages

alumina particles during the milling process. Therefore, the crisp particles of Al_2O_3 are broken and become smaller by rising the work hardening [35].

The long milling time due to high cold working (90 h) results in the dissolution of chromium in the copper matrix. Moreover, the dissolution of Cr in the structure was increased at high chromium proportions, thereby fracturing and crisping of Cu parties were performed. In addition, intense work-hardening leads to the formation of micro-cracks and motion-less dislocations, because of the BCC crystallographic structure of Cr. The other micro-cracks will be created at the margin of the particles. Cr powders will be spread in the matrix and induce these micro-cracks to develop and open [36]. So,

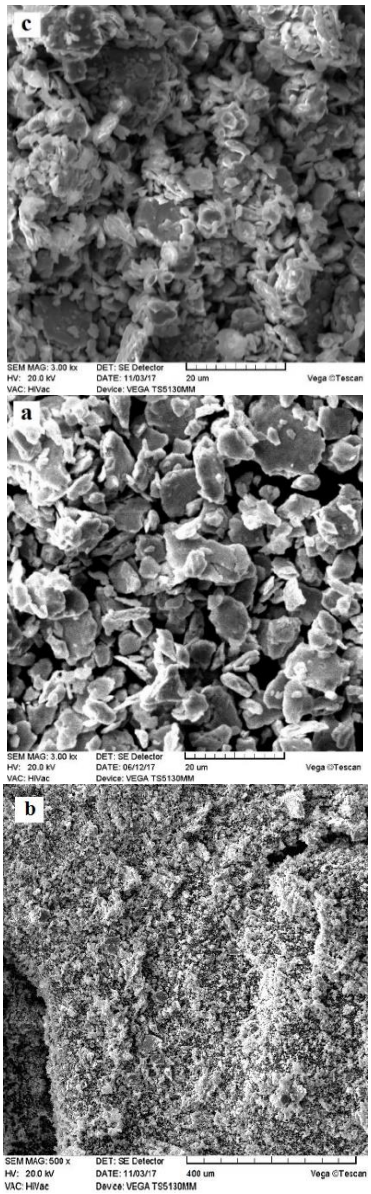

Figure 4. SEM images of Cu-Cr alloys with 1, 3, and 6 weight percentages

it can be assumed that the higher percentage of chromium results in the smaller Cr composite particles at the same activation time. Finally, fine and uniform morphology is acquired by repeated fractures.

Likewise, the particle size distribution of copper-titanium alloys is reduced and they also became agglomerated because of the long activating time (90 h) and creation of a balance between fracture and cold welding. The hexagonal close-packed (HCP) crystal structures of Ti particles are trapped between Cu powders with the face-centered cubic (FCC) structures, which have a more quick work-hardening than Cu [37]. At the current step, the higher fragile Ti powders are spread into the smoother Cu powders and they generate small cracks in their margins which significantly decreases the mechanical properties of the composites [36].

Figure 3 shows SEM images of Cu-Al_2O_3 samples with 1, 3, and 6 weight percentages. SEM images of Cu-Cr alloys with 1, 3, and 6 weight percentages is shown in Figure 4. Also, Figure 5 depicts SEM images of Cu-Ti alloys with 1, 3, and 6 weight percentages.

The micro-hardness of the products after the heat treatment is represented in Figure 6. Cu-1wt%Al_2O_3 and Cu-6wt%Ti had the lowest and highest micro-hardness, respectively. It is worth noting that the inserted forces during the pressing stage did not cause a major change in the hardness of specimens. This is because of an extensive cold hardening of the particle during the process [36].

The number of vacancies and dislocations declined significantly after the annealing procedure. This process is similar to solid solutions, which decomposed after the heat treatment step [38]. Hence, porosity, grain boundaries, and particles of alloying elements are the main reasons for residual resistivity.

By enhancement in the percentage of the second phase, the hardness of all Cu-based composites was raised. As mentioned previously, the enhancement volume of alloying elements causes a boost in the lattice constant and strength of nanocomposites. A higher proportion in reinforcement materials, richer solid solution, and a higher density of dislocations result in Cu cold working and as a result, micro-hardness of the composites was improved. On the one hand, a high amount of coherent precipitates will be created because of the high content of a solid solution in aging. On the other, defects create favored areas to precipitate. Therefore, generated precipitates inhibit the recrystallization and recovery.

Ti has low solvability in Cu at ambient temperature (less than 0.1% of atomic weight) [39]. During the MA process, the density of Ti in the Cu lattice is raised and attained a balance status. The created Ti super-saturation in the copper matrix via mechanical alloying and sintering presents an appropriate condition for the fabrication of Ti with a nano-scale structure.

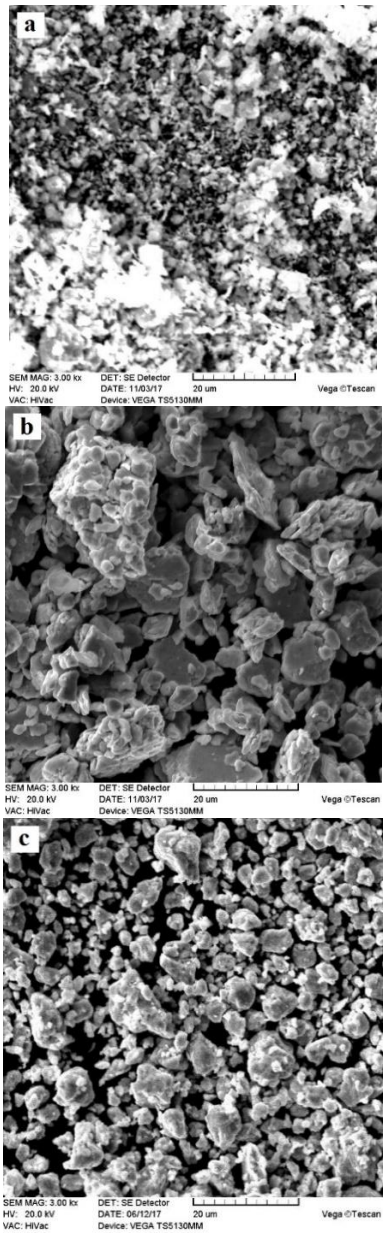

Figure 5. SEM images of Cu-Ti alloys with 1, 3, and 6 weight percentages

Subsequently, the creation of the rich titanium particles in the Cu lattice at the annealing stage coincides with the recovery and recrystallization. This phenomenon frequently ceased the softening procedure. Formed Cu_4Ti at the beginning steps of heat treatment is in the shape of uniform nanostructures [40]. The mentioned precipitates are produced inside the grain boundaries [41] and they act as obstacles to dislocation movements. As a result, they will delay recovery and recrystallization, and the micro-hardness of nanocomposites will be increased.

Similar to Cu-Ti, the mentioned hardening mechanism is valid for Cu-Cr and Cu-Al alloys and so

the second phase rises the heat of recrystallization and postpones the recrystallization and recovery. Uniform precipitation of copper-chromium and copper-aluminum that was created at the aging step, causes the halt of re-crystallization and rises the strength. The maximum hardness in copper-based composites is achievable if all of the effective variables in the milling and annealing steps are performed accurately. Figure 7 indicates the schematic diagram of the ideal Cu-based nanocomposites with homogenous dispersion of nano-sized particles in the grains.

4. 1. ANN Architecture There is no general rule to determine the minimum or the maximum number of required datasets in an ANN network [42]. However, it seems the model needs a reasonable number of data to avoid under-training or over-training. Here, 12 and 85 data were used for verification and training of the model, respectively.

FFBPNN was used for the learning module. Feed-forward back propagation neural network is a specific type of ANN with many capabilities to attain favorable outcomes and is extensively applied in the MA to participate in major variables in previous works [43-45]. There are two steps per turn of the process in FFBPNN.

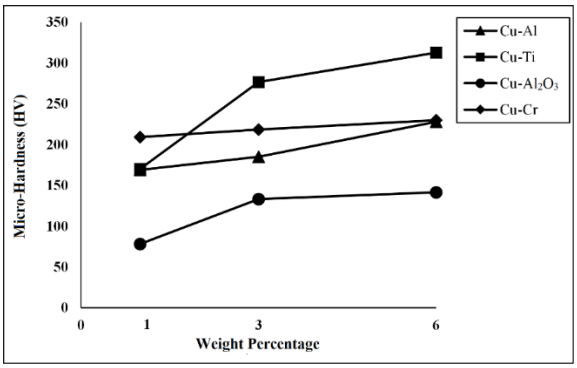

Figure 6. The micro-hardness of the Cu-based composites at different weight percentages of alloying element

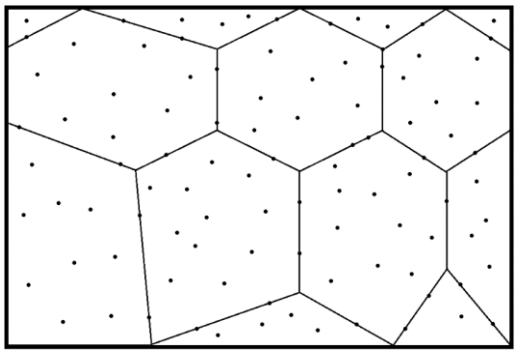

Figure 7. Schematic illustration of an ideal nano-dispersed of the second phase particles to achieve the maximum strength in the Cu-based nanocomposites

First is the specification of a random number for all weight factors which is the feed-forward. Next, altering the weights to reach the outcome with lower error and closer to the actual quantity which is the back-propagation. The cycle is done frequently till the outcome of the model reaches the closest actual value for all of the training data [46, 47].

Basically, there is no straightforward way to optimize the structure of an ANN model [29]. For the effective function of the network, various learning architectures have been applied to assess the structure of the network during the learning step. The created model includes two hidden layers with input and output layers. The hidden layers include 12 and 8 neurons in the first and second layers, respectively. Input parameters were the hardness, volume, and size of reinforcements, BPR, speed and time of ball-milling, and the initial size. As well as, the hardness of the nanocomposite was the output. Figure 8 shows the graphical abstract of the designed ANN.

In order to compute the regression, the finite element method and the trained model were applied. The regression is illustrated in Table 1. Regarding the regression, “Tansig”, “Purelin”, and “Logsig” are the finest functions for the hidden layers (1st and 2nd) and output layer, respectively (number 10). Obviously, trial and error do not follow a general pattern. As a result, it needs to train the network several times to reach an acceptable error without any specific approach. The trial and error strategy is used vastly in other similar studies in order to find a more suitable network structure and decrease the regression [48, 49].

To design the network, MATLAB (2014) owing to its user-friendly was used. Moreover, the Levenberg–Marquardt algorithm due to rapid training ability was employed for training the model. In addition, the log-sigmoid activation function was utilized as the transfer function. This is a non-linear and S-shaped function which is defined according to Equation (2):

$$f(x) = \frac{1}{1+e^{-x}} \quad (2)$$

The collected data had been normalized and homogenized (0.1-0.9) according to Equation (3):

$$\mathrm{N} = 0.8\left(\frac{x-x_{min}}{x_{max}-x_{min}}\right) + 0.1 \quad (3)$$

RMSE is defined as the standard deviation of the differences between the actual and predicted values. Here, the RMSE of the model was calculated using Equation (4):

$$\mathrm{RMSE} = \frac{1}{\mathrm{N}}\sum_{1}^{\mathrm{N}}\left(\frac{|\text{True value}-\text{Predicted value}|}{\text{True value}} \times 100\right) \quad (4)$$

4. 2. ANN Results Regression analysis was performed for testing the precision of the designed network. Figure 9 illustrates the result of the regression analysis. Based on Figure 9, the general regression is

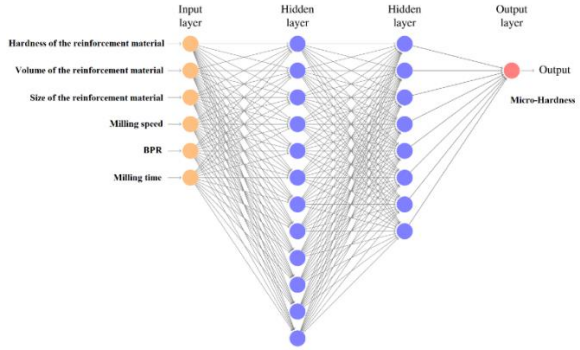

Figure 8. Architecture of the designed ANN

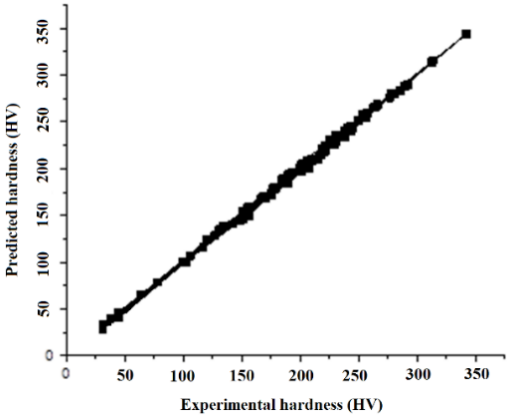

Figure 9. The regression of the ANN model

TABLE 1. The values of regressions for different ANN structures

No.	Transfer function			Nodes in hidden layers		Regression (R^2)
	Hidden layers		Output layer	Layer two	Layer one	
	Layer two	Layer one				
1	Tansig	Tansig	Tansig	16	12	0.8843
2	Tansig	Logsig	Purelin	12	7	0.7634
3	Logsig	Logsig	Tansig	3	5	0.6674
4	Logsig	Logsig	Logsig	7	5	0.4219
5	Logsig	Logsig	Purelin	9	6	0.7396
6	Logsig	Tansig	Logsig	3	7	0.5732
7	Tansig	Tansig	Tansig	16	12	0.9318
8	Tansig	Logsig	Purelin	12	7	0.8843
9	Logsig	Logsig	Tansig	3	5	0.7634
10*	Tansig	Purelin	Logsig	12	8	0.9914

*Best ANN structure

TABLE 2. Comparison of the actual and predicted values for different Cu-based nanocomposites

Experimental Micro-Hardness (HV)	Anticipated Micro-Hardness (HV)	Samples
169	171	Cu-1wt%Al
185	183	Cu-3wt%Al
228	232	Cu-6wt%Al
78	89	Cu-1wt%Al_2O_3
133	143	Cu-3wt%Al_2O_3
141	153	Cu-6wt%Al_2O_3
209	210	Cu-1wt%Cr
218	219	Cu-3wt%Cr
229	228	Cu-6wt%Cr
170	175	Cu-1wt%Ti
276	276	Cu-3wt%Ti
312	293	Cu-6wt%Ti

0.9914. The result of the regression graph shows that there is a good fit between experimental hardness and predicted hardness. Therefore, the network model is prepared to anticipate the micro-hardness of copper composites with a reasonable percentage of error.

For verification of the generated model, a comparison between experimental and predicted data was performed. The error of the network was calculated by 3.7% regarding Equation (4). Table 2 indicates the actual and anticipated values for the micro-hardness of the different Cu nanocomposites. The validation results confirm that created network is reliable and with high accuracy anticipates the experimental values of the micro-hardness. As a consequence, it can be assumed that the designed ANN could predict another similar study with such high reliability and approximation. Additionally, the created model results in a more proximate evaluation of lab-based works, due to several major variables in mechanical alloying and the complexity of coordinating and launching them.

5. CONCLUSION

1. The morphology of Cu-based alloys was fundamentally different from each other and tends to be smaller particles via the rising volume of the reinforcement materials. Adding Al_2O_3 to the Cu matrix forms a sheet-like morphology; while adding aluminum, chromium, and titanium leads to homogeneous morphology in Cu-based composites .
2. The hardness of the alloys was raised via the enhancement in the percentage of the second phase. Al_2O_3 and Ti had the lowest and highest impact on the micro-hardness, respectively.

3. The FFBPNN with 12 and 8 neurons in the first and second hidden layers, respectively, is an efficient approach for the anticipation of the microhardness of Cu nanocomposites produced via mechanical alloying.
4. To design a reliable ANN architecture, “Tansig”, “Purelin”, and “Logsig” are the favourable activation functions for the hidden layers (1st and 2nd), and output layer, respectively.
5. RMSE of the proposed network for prediction of the micro-hardness of Cu nanocomposites was 3.7%.

6. REFERENCES

1. Saindane, U., Soni, S. and Menghani, J., "Dry sliding behavior of carbon-based brake pad materials", ***International Journal of Engineering***, Vol. 34, No. 11, (2021), 2517-2524. doi: 10.5829/IJE.2021.34.11B.14.
2. Saindane, U., Soni, S. and Menghani, J., "Performance evaluation of brake pads developed using two different manufacturing methods", ***Materialwissenschaft und Werkstofftechnik***, Vol. 54, No. 2, (2023), 186-195. https://doi.org/10.1002/mawe.202100407
3. Asgharian Marzabad, M., Jafari, B. and Norouzi, P., "Determination of riboflavin by nanocomposite modified carbon paste electrode in biological fluids using fast fourier transform square wave voltammetry", ***International Journal of Engineering, Transactions C: Aspects***, Vol. 33, No. 9, (2020), 1696-1702. doi: 10.5829/IJE.2020.33.09C.01.
4. Pellizzari, M. and Cipolloni, G., "Tribological behaviour of cu based materials produced by mechanical milling/alloying and spark plasma sintering", ***Wear***, Vol. 376, (2017), 958-967. https://doi.org/10.1016/j.wear.2016.11.050
5. Torabi, A., Babaheydari, R., Akbari, G. and Mirabootalebi, S., "Optimizing of micro-hardness of nanostructured cu–cr solid solution produced by mechanical alloying using ann and genetic algorithm", ***SN Applied Sciences***, Vol. 2, No. 11, (2020), 1-9. https://doi.org/10.1007/s42452-020-03722-x
6. Fathy, A., Wagih, A. and Abu-Oqail, A., "Effect of zro2 content on properties of cu-zro2 nanocomposites synthesized by optimized high energy ball milling", ***Ceramics International***, Vol. 45, No. 2, (2019), 2319-2329. https://doi.org/10.1016/j.ceramint.2018.10.147
7. Abu-Oqail, A., Samir, A., Essa, A., Wagih, A. and Fathy, A., "Effect of gnps coated ag on microstructure and mechanical properties of cu-fe dual-matrix nanocomposite", ***Journal of Alloys and Compounds***, Vol. 781, (2019), 64-74. https://doi.org/10.1016/j.jallcom.2018.12.042
8. Eze, A.A., Jamiru, T., Sadiku, E.R., Durowoju, M.O., Kupolati, W.K., Ibrahim, I.D., Obadele, B.A., Olubambi, P.A. and Diouf, S., "Effect of titanium addition on the microstructure, electrical conductivity and mechanical properties of copper by using sps for the preparation of cu-ti alloys", ***Journal of Alloys and Compounds***, Vol. 736, (2018), 163-171. https://doi.org/10.1016/j.jallcom.2017.11.129.
9. Babaheydari, R., Mirabootalebi, S. and Akbari, G., "Investigation on mechanical and electrical properties of cu-ti nanocomposite produced by mechanical alloying", ***International Journal of Engineering, Transactions C: Aspects***, Vol. 33, No. 9, (2020), 1759-1765. doi: 10.5829/IJE.2020.33.09C.09.
10. Alex, S., Chattopadhyay, K., Barshilia, H.C. and Basu, B., "Thermally evaporated cu–al thin film coated flexible glass mirror for concentrated solar power applications", ***Materials Chemistry and Physics***, Vol. 232, (2019), 221-228. https://doi.org/10.1016/j.matchemphys.2019.04.078
11. Hussain, M., Khan, U., Jangid, R. and Khan, S., "Hardness and wear analysis of cu/Al_2O_3 composite for application in edm electrode", in IOP Conference Series: Materials Science and Engineering, IOP Publishing. Vol. 310, (2018), 012044.
12. De Marco, V., Grazioli, A. and Sglavo, V.M., "Production of planar copper-based anode supported intermediate temperature solid oxide fuel cells cosintered at 950 c", ***Journal of Power Sources***, Vol. 328, (2016), 235-240. https://doi.org/10.1016/j.jpowsour.2016.08.025
13. Saha, S., Abd Hamid, S.B. and Ali, T.H., "Catalytic evaluation on liquid phase oxidation of vanillyl alcohol using air and H_2O_2 over mesoporous cu-ti composite oxide", ***Applied Surface Science***, Vol. 394, (2017), 205-218. https://doi.org/10.1016/j.apsusc.2016.10.070
14. Shen, D., Zhu, Y., Yang, X. and Tong, W., "Investigation on the microstructure and properties of cu-cr alloy prepared by in-situ synthesis method", ***Vacuum***, Vol. 149, (2018), 207-213. https://doi.org/10.1016/j.vacuum.2017.12.035
15. Gustmann, T., Dos Santos, J., Gargarella, P., Kühn, U., Van Humbeeck, J. and Pauly, S., "Properties of cu-based shape-memory alloys prepared by selective laser melting", ***Shape Memory and Superelasticity***, Vol. 3, No. 1, (2017), 24-36. https://doi.org/10.1007/s40830-016-0088-6.
16. Li, J., Chang, L., Li, S., Zhu, X. and An, Z., "Microstructure and properties of as-cast cu-cr-zr alloys with lanthanum addition", ***Journal of Rare Earths***, Vol. 36, No. 4, (2018), 424-429. https://doi.org/10.1016/j.jre.2017.11.006
17. Vorotilo, S., Loginov, P.A., Churyumov, A.Y., Prosviryakov, A.S., Bychkova, M.Y., Rupasov, S.I., Orekhov, A.S., Kiryukhantsev-Korneev, P.V. and Levashov, E.A., "Manufacturing of conductive, wear-resistant nanoreinforced cu-ti alloys using partially oxidized electrolytic copper powder", ***Nanomaterials***, Vol. 10, No. 7, (2020), 1261. https://doi.org/10.3390/nano10071261
18. Agboola, P.O., Shakir, I., Almutairi, Z.A. and Shar, S.S., "Hydrothermal synthesis of cu-doped cos2@ nf as high performance binder free electrode material for supercapacitors applications", ***Ceramics International***, Vol. 48, No. 6, (2022), 8509-8516. https://doi.org/10.1016/j.ceramint.2021.12.061
19. Rodak, K., "Cu-cr and cu-fe alloys processed by new severe plastic deformation: Microstructure and properties", ***Severe Plastic Deformation Techniques***, (2017), 115. doi: 10.5772/intechopen.68954.
20. Awadallah, O. and Cheng, Z., "Formation of sol-gel based cu2znsns4 thin films using ppm-level hydrogen sulfide", ***Thin Solid Films***, Vol. 625, (2017), 122-130. https://doi.org/10.1016/j.tsf.2017.01.054
21. Liau, L.C.-K. and Huang, J.-S., "Energy-level variations of cu-doped zno fabricated through sol-gel processing", ***Journal of Alloys and Compounds***, Vol. 702, (2017), 153-160. https://doi.org/10.1016/j.jallcom.2017.01.174
22. Hosseini, M., Pardis, N., Manesh, H.D., Abbasi, M. and Kim, D.-I., "Structural characteristics of cu/ti bimetal composite produced by accumulative roll-bonding (ARB)", ***Materials & Design***, Vol. 113, (2017), 128-136. https://doi.org/10.1016/j.matdes.2016.09.094
23. Cheng, J., Cai, Q., Zhao, B., Yang, S., Chen, F. and Li, B., "Microstructure and mechanical properties of nanocrystalline al-zn-mg-cu alloy prepared by mechanical alloying and spark plasma sintering", ***Materials***, Vol. 12, No. 8, (2019), 1255. https://doi.org/10.3390/ma12081255
24. Mirabootalebi, S. and Akbari, G., "Phase transformation in carbon during mechanical alloying of graphite: Experimental and

molecular dynamic study", ***Journal of Materials Engineering and Performance***, (2022), 1-11. https://doi.org/10.1007/s11665-022-07706-3

25. Mirabootalebi, S.O., "Experimental and molecular dynamic studies of phase transformation and amorphization in silicon during high-energy ball milling", ***Materials Today: Proceedings***, Vol. 76, (2023), 607-615. https://doi.org/10.1016/j.matpr.2022.12.098.
26. Mirabootalebi, S. and Babaheydari, R., "Prediction length of carbon nanotubes in cvd method by artificial neural network", ***Iran JOC***, Vol. 11, No. 4, (2019), 2731.
27. Majumder, H. and Maity, K., "Multi-response optimization of wedm process parameters using taguchi based desirability function analysis", in IOP Conference Series: Materials Science and Engineering. IOP Publishing. (2018).
28. Saindane, U., Soni, S. and Menghani, J., "Friction and wear performance of brake pad and optimization of manufacturing parameters using grey relational analysis", ***International Journal of Engineering, Transactions C: Aspects***, Vol. 35, No. 3, (2022), 552-559. doi: 10.5829/IJE.2022.35.03C.07.
29. Shaikh, R., Shirazian, S. and Walker, G.M., "Application of artificial neural network for prediction of particle size in pharmaceutical cocrystallization using mechanochemical synthesis", ***Neural Computing and Applications***, Vol. 33, No. 19, (2021), 12621-12640. https://doi.org/10.1007/s00521-021-05912-z
30. Babaheydari, R. and Mirabootalebi, S., "Prediction micro-hardness of al-based composites by using artificial neural network in mechanical alloying", ***Journal of Environmental Friendly Materials***, Vol. 4, No. 1, (2020), 31-35.
31. Petrudi, A.M. and Rahmani, M., "Validation and optimization of thermophysical properties for thermal conductivity and viscosity of nanofluid engine oil using neural network", ***Journal of Modeling and Simulation of Materials***, Vol. 3, No. 1, (2020), 53-60. https://doi.org/10.21467/jmsm.3.1.53-60
32. Da Silva, I.N., Spatti, D.H., Flauzino, R.A., Liboni, L.H.B. and dos Reis Alves, S.F., Artificial neural network architectures and training processes, in Artificial neural networks. 2017, Springer.21-28.
33. Mirahmadi Babaheydari, R., Mirabootalebi, S.O. and Akbari Fakhrabadi, G.H., "Effect of alloying elements on hardness and electrical conductivity of cu nanocomposites prepared by mechanical alloying", ***Iranian Journal of Materials Science and Engineering***, Vol. 18, No. 1, (2021), 1-11. doi: 10.22068/ijmse.18.1.1.
34. Mirabootalebi, S., "A new method for preparing buckypaper by pressing a mixture of multi-walled carbon nanotubes and amorphous carbon", ***Advanced Composites and Hybrid Materials***, Vol. 3, (2020), 336-343. https://doi.org/10.1007/s42114-020-00167-z
35. Safi, S. and Akbari, G., "Evaluation of synthesizing al2o3 nano particles in copper matrix by mechanical alloying of cu-1% al and copper oxide", ***Journal of Advanced Materials in Engineering (Esteghlal)***, Vol. 36, No. 1, (2017), 71-85. doi: 10.18869/ACADPUB.JAME.36.1.71.
36. Suryanarayana, C., "Mechanical alloying and milling", ***Progress in Materials Science***, Vol. 46, No. 1-2, (2001), 1-184. https://doi.org/10.1016/S0079-6425(99)00010-9
37. Pourfereidouni, A. and Akbari, G.H., "Development of nano-structure cu-ti alloys by mechanical alloying process", in Advanced Materials Research. Vol. 829, (2013), 168-172.
38. Wang, Y., Bossé, G., Nair, H., Schreiber, N., Ruf, J., Cheng, B., Adamo, C., Shai, D., Lubashevsky, Y. and Schlom, D., "Subterahertz momentum drag and violation of matthiessen's rule in an ultraclean ferromagnetic srruo 3 metallic thin film", ***Physical Review Letters***, Vol. 125, No. 21, (2020), 217401. https://doi.org/10.1103/PhysRevLett.125.217401
39. Murray, J., "The cu− ti (copper-titanium) system", ***Bulletin of Alloy Phase Diagrams***, Vol. 4, No. 1, (1983), 81-95. https://doi.org/10.1007/BF02880329
40. Datta, A. and Soffa, W., "The structure and properties of age hardened cu-ti alloys", ***Acta Metallurgica***, Vol. 24, No. 11, (1976), 987-1001. https://doi.org/10.1016/0001-6160(76)90129-2
41. Lopez-Hirata, V.M., Hernandez-Santiago, F., Saucedo-Muñoz, M.L., Avila-Davila, E.O. and Villegas-Cardenas, J.D., Analysis of β′(cu 4 ti) precipitation during isothermal aging of a cu–4 wt% ti alloy, in Characterization of minerals, metals, and materials 2020. 2020, Springer.403-412.
42. Akinwekomi, A.D. and Lawal, A.I., "Neural network-based model for predicting particle size of az61 powder during high-energy mechanical milling", ***Neural Computing and Applications***, Vol. 33, No. 24, (2021), 17611-17619. https://doi.org/10.1007/s00521-021-06345-4
43. Varol, T. and Ozsahin, S., "Artificial neural network analysis of the effect of matrix size and milling time on the properties of flake al-cu-mg alloy particles synthesized by ball milling", ***Particulate Science and Technology***, Vol. 37, No. 3, (2019), 381-390. https://doi.org/10.1080/02726351.2017.1381658.
44. Varol, T., Canakci, A. and Ozsahin, S., "Prediction of effect of reinforcement content, flake size and flake time on the density and hardness of flake aa2024-sic nanocomposites using neural networks", ***Journal of Alloys and Compounds***, Vol. 739, (2018), 1005-1014. https://doi.org/10.1016/j.jallcom.2017.12.256
45. Devadiga, U., Poojary, R.K.R. and Fernandes, P., "Artificial neural network technique to predict the properties of multiwall carbon nanotube-fly ash reinforced aluminium composite", ***Journal of Materials Research and Technology***, Vol. 8, No. 5, (2019), 3970-3977. https://doi.org/10.1016/j.jmrt.2019.07.005
46. Panda, S. and Panda, G., "Performance evaluation of a new bp algorithm for a modified artificial neural network", ***Neural Processing Letters***, (2020), 1-21. https://doi.org/10.1007/s11063-019-10172-z.
47. Mirabootalebi, S.O., Fakhrabadi, G.H.A. and Mirahmadi, R., "Carbon via ball milling of graphite and prediction of its crystallite size through ann", ***Organomet. Chem***, Vol. 1, No. 2, (2021), 76-85. http://dx.doi.org/10.22034/jaoc.2021.288020.1021
48. Zhou, G., Moayedi, H., Bahiraei, M. and Lyu, Z., "Employing artificial bee colony and particle swarm techniques for optimizing a neural network in prediction of heating and cooling loads of residential buildings", ***Journal of Cleaner Production***, Vol. 254, (2020), 120082. https://doi.org/10.1016/j.jclepro.2020.120082
49. Moayedi, H., Tien Bui, D., Gör, M., Pradhan, B. and Jaafari, A., "The feasibility of three prediction techniques of the artificial neural network, adaptive neuro-fuzzy inference system, and hybrid particle swarm optimization for assessing the safety factor of cohesive slopes", ***ISPRS International Journal of Geo-Information***, Vol. 8, No. 9, (2019), 391. https://doi.org/10.3390/ijgi8090391

Persian Abstract

چکیده

نانوکامپوزیت‌های بر پایه مس یکی از پرطرفدارترین مواد در توزیع برق، صنعت جوش، تجهیزات هیدرولیک، ماشین آلات صنعتی و غیره می باشند. در میان روش های مختلف برای ساخت آلیاژهای مس، آلیاژ مکانیکی (MA) رویکرد اصلی است .که این روش ساده، ارزان، مناسب برای تولید انبوه است و ظرفیت بالایی برای توزیع همگن فاز دوم دارد .با این حال، پیش‌بینی سختی محصولات در MA به دلیل وجود پارامترهای مؤثر بسیار دشوار است .در این کار، ما یک شبکه عصبی انتشار برگشتی پیش‌خور (FFBPNN) برای پیش‌بینی سختی نانوکامپوزیت‌های مبتنی بر مس طراحی کردیم .ابتدا، برخی از رایج‌ترین نانوکامپوزیت‌های مس از جملهCu-Al ، Cu-Al2O3، Cu-Crو Cu-Ti با آلیاژ مکانیکی مس در درصدهای وزنی متفاوت (۱، ۳ و ٦) سنتز شدند .سپس پودرهای آلیاژی توسط پرس سرد (۱۲ تن) متراکم شده و تحت عملیات حرارتی در دمای ٦٥٠ درجه سانتیگراد قرار گرفتند .سپس استحکام آلیاژها با تست میکروسکوپ ویکرز اندازه گیری شد .در نهایت، برای پیش‌بینی ریزسختی نانوکامپوزیت‌های مس، متغیرهای مهم در فرآیند آسیاب گلوله‌ای شامل سختی، اندازه و حجم مواد تقویت‌کننده، سرعت ویال، نسبت وزنی توپ به پودر (BPR) و زمان آسیاب؛ به عنوان ورودی تعیین شد و سختی نانوکامپوزیت به عنوان خروجی شبکه عصبی مصنوعی (ANN) در نظر گرفته شد .برای آموزش شبکه عصبی مصنوعی، بسیاری از معماری های شبکه عصبی مصنوعی مختلف به کار گرفته شده است و ساختار بهینه مدل با رگرسیون ۰/۹۹۱٤ به دست آمد .این شبکه با دو لایه مخفی طراحی شده است .لایه پنهان اول و دوم به ترتیب شامل ۱۲ و ۸ نورون است .مقایسه بین نتایج پیش‌بینی‌شده شبکه و مقادیر تجربی نشان داد که مدل پیشنهادی با ریشه میانگین مربعات خطا 3.7 (RMSE) درصد می‌تواند ریزسختی نانوکامپوزیت‌ها را پیش‌بینی کند.